

PAPER

Elastic scattering of electrons from the ions of argon isonuclear series


To cite this article: Mahmudul H Khandker *et al* 2019 *Phys. Scr.* **94** 075402

View the [article online](#) for updates and enhancements.

You may also like

- [Nucleon-nucleus optical potential computed with the Gogny interaction](#)
Juan Lopez-Moraña and Xavier Viñas
- [Elastic scattering of electrons by Sr atom: a study of critical minima and spin polarization](#)
Ashok Kumar, M N A Abdullah, A K F Haque et al.
- [A study of the critical minima and spin polarization in the elastic electron scattering by the lead atom](#)
A K F Haque, M M Haque, M Sohag Hossain et al.

Elastic scattering of electrons from the ions of argon isonuclear series

Mahmudul H Khandker¹, A K F Haque^{1,2}, M Maaza^{2,3} and M Alfaz Uddin^{1,4} 

¹Department of Physics, University of Rajshahi, Rajshahi-6205, Bangladesh

²Nanosciences African network (NANOAFNET), Materials Research Group (MRG), iThemba LABS-National Research Foundation (NRF), 1 Old Faure Road, 7129, PO Box 722, Somerset West, Western Cape Province, South Africa

³UNESCO-UNISA Africa Chair in Nanosciences/Nanotechnology Laboratories, College of Graduate Studies, University of South Africa (UNISA), Muckleneuk Ridge, PO Box 392, Pretoria, South Africa

E-mail: uddinmda@yahoo.com

Received 30 January 2019, revised 23 February 2019

Accepted for publication 6 March 2019

Published 16 April 2019



Abstract

Absolute angular differential, integrated elastic and momentum transfer cross-sections for elastically scattered electrons from the ions ($\text{Ar}^+ - \text{Ar}^{18+}$) of argon isonuclear series, over the energy range 3.3–100 eV, are calculated employing a complex electron-ion optical potential within the framework of Dirac relativistic partial wave analysis. The cross sections are analyzed in terms of the contributions from pure Coulomb field and the short range electron-ion complex optical potential comprising static, exchange, correlation-polarization and absorption potentials. Comparison of our calculations with the available experimental data and other theoretical calculations shows a satisfactory agreement.

Keywords: scattering of electrons, cross sections, argon ions, multiply charged ions, modified Coulomb field, Dirac partial wave analysis

(Some figures may appear in colour only in the online journal)

1. Introduction

Electron-ion scattering has both fundamental and practical (economic) importance. The collision data are not only used for unraveling electron-ion interactions, but also in such applied areas as microdosimetry, radiation dosimetry, nuclear medicine, radiation therapy and protection, various electron spectroscopic technologies, etc. The electron-ion elastic scattering data are also immensely needed in understanding behaviors of plasmas occurring in solar corona, astrophysical objects, atmosphere, gas discharges, fusion plasmas, x-ray lasers, etc [1, 2]. In passage through matter such as argon discharge tube, other laboratory and astrophysical plasmas, etc the electron is not only scattered, but also produces ions of different charges. The knowledge of state of ionization, time evolution of the changes and light emission, etc need electron ion collision data for understanding the behavior of the plasmas. Experimental advances and recent availability of intense sources of multiply charged ions opens the possibility of measuring angular

scattering of electrons from multiply positive charged ions. These outpour of experimental data and demand for collision data have stimulated theoretical studies on electron-ion scattering.

Greenwood *et al* [3] measured the absolute angular differential cross section (DCS) for large angle scattering of a free electron by Ar^+ at 3.3 eV. Brotton *et al* [2] presented the measured DCS values for the elastic scattering of electrons from Ar^+ at the collision energy of 16 eV along with their partial wave calculations for the same. McKenna and Williams [4] reported the experimental DCS for elastic scattering of electrons from Ar^{2+} at 16 eV using a crossed-beam energy-loss spectrometer and compared these with their own calculations. Srigengan *et al* [5] publish the experimental DCS data and partial wave calculations based on a semi-empirical potential for the electron scattering from Ar^{2+} and Ar^{3+} at 16 eV. Using a 150° cross beam method, Wang *et al* [6] measured the DCS of electrons elastically scattered from Ar^{7+} at 100 eV. Bélenger *et al* [7] reported the DCS for the elastic scattering of electrons from Ar^{8+} at 12.98 and 22.46 eV at scattering angles between 32° and 148°.

⁴ Author to whom any correspondence should be addressed.

The literature is rife with theoretical studies on the scattering of electron and positron from rare gas atoms. Among these, are the calculations of McEachran and Stauffer [8], Chen *et al* [9], Bartschat *et al* [10], Green *et al* [11] and Fursa and Bray [12]. But theoretical studies of electron or positron scattering from ions are not so many. Shefered and Dickinson [13] predicted DCSs for the elastic scattering of electrons from Ar^{8+} using model potential and quantum defect method at energies 12.98 and 22.46 eV. Nishikawa *et al* [14] calculated DCSs of elastically scattered electrons from Ar^{7+} at 20, 50 and 100 eV with the R-matrix method.

Motivated by the collision data need and refinement of electron-ion interaction and collision dynamics, this work has undertaken the theoretical investigation of electron-ion scattering. In particular, in a glow discharge tube using argon atom, ions of the argon isonuclear series are formed. This fact interests us to study electron scattering from all the ions of argon. This work covered all the ions of argon isonuclear series for the elastic scattering of electrons in an objective of getting insight into the charge dependence of various cross-sections of the ions. This work employs a short range electron-ion optical potential arising from the interaction of bound electrons with the nuclear charge distribution in conjunction with the pure form of long range Coulomb field due to the net ionic charge. The complex electron-ion optical potential has both real and imaginary parts. The real part consists of static, exchange and correlation-polarization potentials. Electrostatic potential is determined by nuclear and electronic charge distributions of the ions. Rearrangement collisions between projectile electron and bound electrons is handled by replacing the non-local exchange interaction with the approximate local exchange potential. The correlation-polarization potential accounts the polarization of the target charge distribution under the action of projectile's electric field. For energy greater than the first inelastic threshold of the target atom, a loss of projectile flux occurs from elastic channel to inelastic channel. This loss is described by the semi-relativistic negative imaginary potential.

In this work, a complex optical potential, which includes both short range and long range parts, is employed to calculate the DCSs, integrated elastic (IECS) and momentum transfer (MTCS) cross-sections of the ions of argon isonuclear series. The Dirac partial wave analysis is used to carry out the above calculations. The above calculations are carried out over the energy range 3.3–100 eV. Our results are compared with the available experimental data and other theoretical calculations.

The paper is organized as follows. The outline of the theory is given in section 2. In section 3, we provide the discussions of our DCS results with graphs to compare with existing data and calculations. The section 4 contains the conclusion of our findings.

2. Outline of the theory

2.1. The theoretical methodology

The complex optical potential model (OPM) for the electron-ion interaction is represented by a modified Coulomb

potential given as

$$V(r) = \frac{qe^2}{r} + V_{\text{sr}}(r), \quad (1)$$

where q is the ionic charge and $V_{\text{sr}}(r)$ is a short range potential that vanishes at $r > r_c$. With the appropriate normalization of the spherical waves, the upper component radial function takes the asymptotic form for $r \rightarrow \infty$

$$P_{E\kappa}(r) \sim \sin\left(kr - \ell\frac{\pi}{2} - \eta \ln 2kr + \delta_\kappa\right). \quad (2)$$

Here k is the projectiles relativistic wave number, which is related to the kinetic energy E_i by

$$(c\hbar k)^2 = E_i(E_i + 2m_e c^2), \quad (3)$$

κ is the relativistic quantum number defined as $\kappa = (\ell - j)(2j + 1)$, where j and ℓ are the total and orbital angular momentum quantum numbers and δ_κ , the global phase shifts, represent the asymptotic behavior of Dirac spherical waves [15], is given as

$$\delta_\kappa = \Delta_\kappa + \hat{\delta}_\kappa. \quad (4)$$

Here $\hat{\delta}_\kappa$ is the inner phase shift caused by the short range potential and Δ_κ is the Coulomb phase shift of the potential tail that is given by [16]

$$\begin{aligned} \Delta_\kappa = & \arg[\zeta(E_i + 2m_e c^2) \\ & - i(\kappa + \lambda)c\hbar k] - (\lambda - \ell - 1)\frac{\pi}{2} \\ & + \arg \Gamma(\lambda + i\eta) - S(\zeta, \kappa)\pi, \end{aligned} \quad (5)$$

where $\eta = \frac{qe^2 m_e}{\hbar k}$ is the Sommerfeld parameter for Coulomb tail, $\zeta = \frac{qe^2}{\hbar c} \approx \frac{q}{137}$, $\lambda = \sqrt{\kappa^2 - \zeta^2}$, and $S(\zeta, \kappa) = 1$ if $\zeta < 0$ and $\kappa < 0$, and $= 0$ otherwise. The radial equations are integrated from $r = 0$ to a certain distance r_m beyond the range r_c of $V_{\text{sr}}(r)$ to calculate the inner phase shifts $\hat{\delta}_\kappa$. The field becomes purely Coulombian for $r > r_m$ and the normalized upper component radial function can be written as

$$P_{E\kappa}(r) = \cos \hat{\delta}_\kappa f_{E\kappa}^{(u)}(r) + \sin \hat{\delta}_\kappa g_{E\kappa}^{(u)}(r), \quad (6)$$

where $f_{E\kappa}^{(u)}(r)$ and $g_{E\kappa}^{(u)}(r)$ are regular and irregular Dirac-Coulomb functions for $Z = q$. If the radial function $P_{E\kappa}(r)$ and its first derivative are continuous, the inner phase shift $\hat{\delta}_\kappa$ can be determined by matching log derivative of outer analytical form to the inner numerical solution at r_m . This method gives

$$\exp(2i\hat{\delta}_\kappa) = \frac{D_{\text{out}}[f_{E\kappa}^{(u)}(r_m) + i g_{E\kappa}^{(u)}(r_m)] - [(f_{E\kappa}^{(u)})'(r_m) + i (g_{E\kappa}^{(u)})'(r_m)]}{[(f_{E\kappa}^{(u)})'(r_m) - i (g_{E\kappa}^{(u)})'(r_m)] - D_{\text{out}}[f_{E\kappa}^{(u)}(r_m) - i g_{E\kappa}^{(u)}(r_m)]}, \quad (7)$$

where the primes specify the derivatives with respect to r and D_{out} , the logarithmic derivative of the outgoing numerical

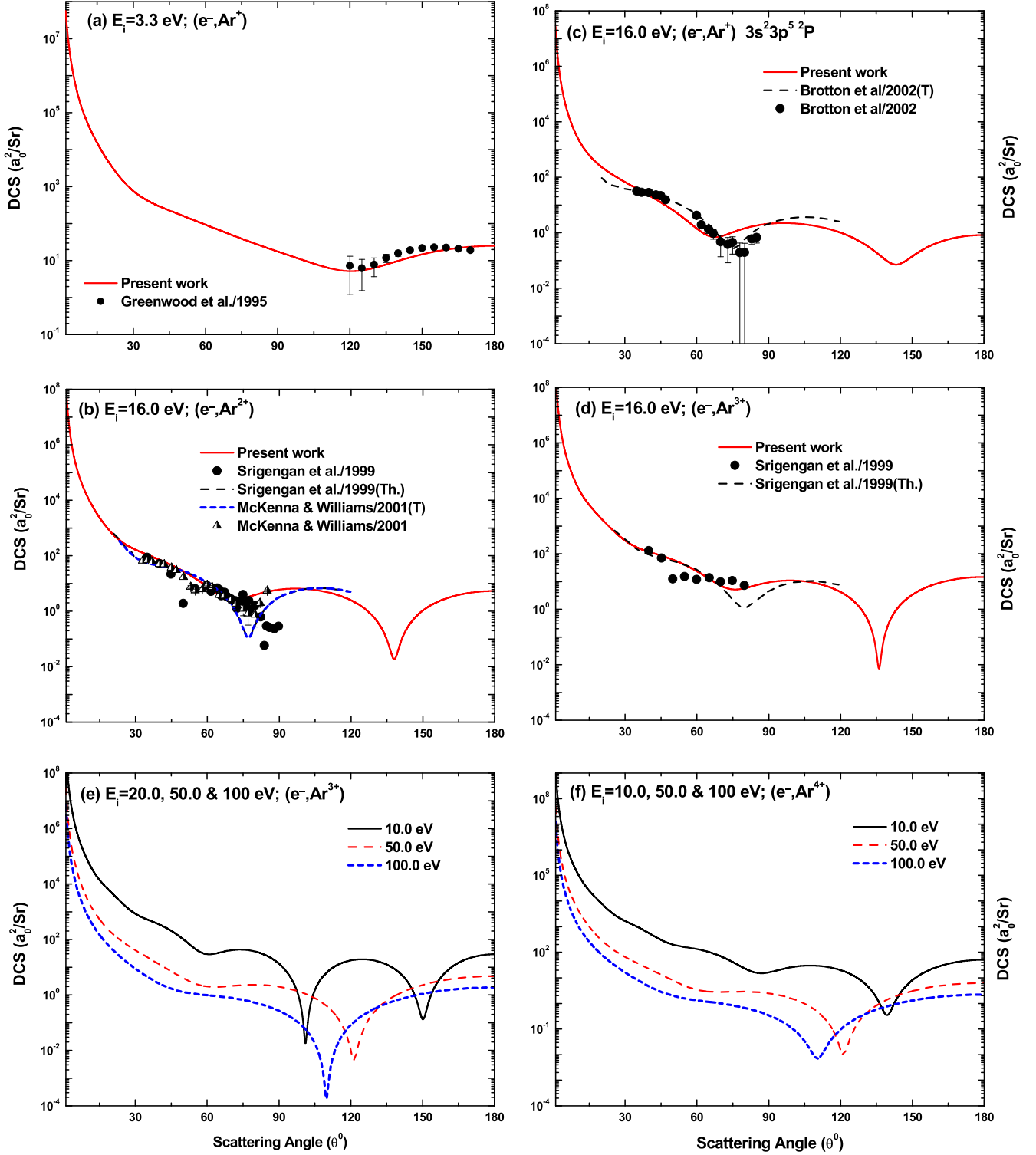


Figure 1. DCS for the elastic scattering of electrons from (a) Ar^+ , $E_i = 3.3$ eV, (b) Ar^+ , $E_i = 16$ eV, (c) Ar^{2+} , $E_i = 16$ eV, (d) Ar^{3+} , $E_i = 16$ eV, (e) Ar^{3+} , $E_i = 10, 50$ and 100 eV and (f) Ar^{4+} , $E_i = 10, 50$ and 100 eV. Theoretical and experimental: Greenwood *et al* [3], Brotton *et al* [2], Srigengan *et al* [5] and McKenna and Williams [4].

radial function at the matching point. If the short range distortion is complex, the phase shift $\hat{\delta}_\kappa$ becomes complex. Clearly, $\hat{\delta}_\kappa$ becomes zero for pure Coulomb field. For

convenience, $f(\theta)$ and $g(\theta)$ can be written as

$$f(\theta) = f_{\text{sr}}(\theta) + f^{(C)}(\theta), \quad g(\theta) = g_{\text{sr}}(\theta) + g^{(C)}(\theta). \quad (8)$$

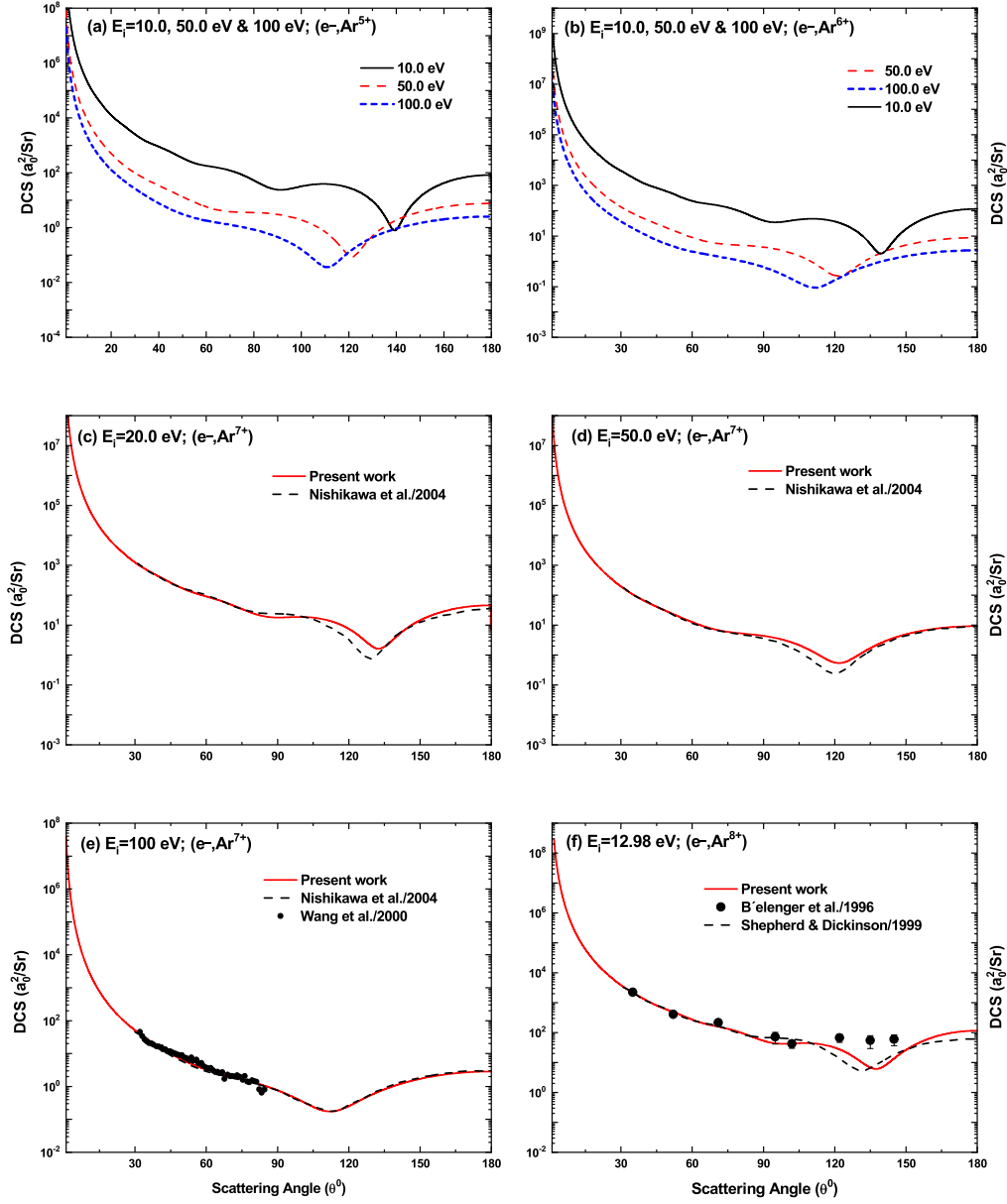


Figure 2. DCS for the elastic scattering of electrons from (a) Ar^{5+} , $E_i = 10, 50$ and 100 eV, (b) Ar^{5+} , $E_i = 10, 50$ and 100 eV, (c) Ar^{7+} , $E_i = 20$ eV, (d) Ar^{7+} , $E_i = 50$ eV, (e) Ar^{7+} , $E_i = 100$ eV and (f) Ar^{8+} , $E_i = 12.98$ eV. Theoretical: Nishikawa *et al* [14] and Shepherd and Dickinson [13]. Experimental: Wang *et al* [6] and B'elenger *et al* [7].

Here $f^{(C)}(\theta)$ and $g^{(C)}(\theta)$, the scattering amplitudes for the Coulomb potential with $Z = q$, are given by

$$f^{(C)}(\theta) = \frac{1}{2ik} \sum_{\ell=0}^{\infty} \{(\ell+1)[\exp(2i\Delta_{-\ell-1}) - 1] + \ell[\exp(2i\Delta_{\ell}) - 1]\} P_{\ell}(\cos\theta) \quad (9)$$

and

$$g^{(C)}(\theta) = \frac{1}{2ik} \sum_{\ell=0}^{\infty} \{\exp(2i\Delta_{\ell}) - \exp(2i\Delta_{-\ell-1})\} P_{\ell}^1(\cos\theta). \quad (10)$$

And $f_{\text{sr}}(\theta)$ and $g_{\text{sr}}(\theta)$, the scattering amplitudes for the short range potential, are given as

$$f_{\text{sr}}(\theta) = \frac{1}{2ik} \sum_{\ell=0}^{\infty} \{(\ell+1)\exp(2i\Delta_{-\ell-1})[\exp(2i\hat{\Delta}_{-\ell-1}) - 1] + \ell \exp(2i\Delta_{\ell})[\exp(2i\hat{\Delta}_{\ell}) - 1]\} P_{\ell}(\cos\theta) \quad (11)$$

and

$$g_{\text{sr}}(\theta) = \frac{1}{2ik} \sum_{\ell=0}^{\infty} \{\exp(2i\Delta_{\ell})[\exp(2i\hat{\Delta}_{\ell}) - 1] - \exp(2i\Delta_{-\ell-1})[\exp(2i\hat{\Delta}_{-\ell-1}) - 1]\} P_{\ell}^1(\cos\theta). \quad (12)$$

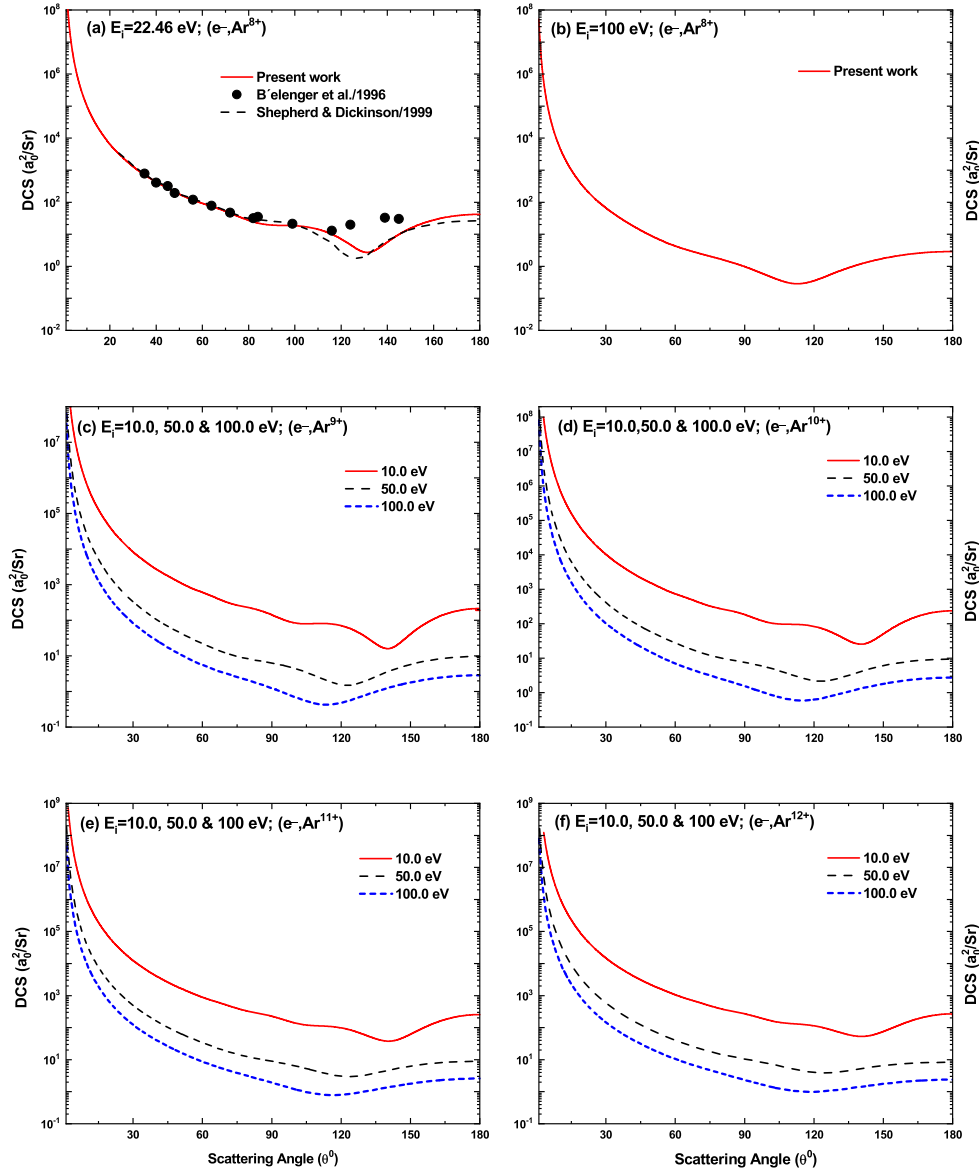


Figure 3. DCS for the elastic scattering of electrons from Ar^{8+} at (a) $E_i = 22.46$ eV, (b) $E_i = 100$ eV and at $E_i = 10, 50$ and 100 eV from (c) Ar^{9+} , (d) Ar^{10+} , (e) Ar^{11+} and (f) Ar^{12+} . Theoretical: Shepherd and Dickinson [13]. Experimental: Bélenger *et al* [7].

The phase shifts δ_{κ} can be obtained numerically from the solution of Dirac relativistic equation [17, 18]. The DCS is then given by

$$\frac{d\sigma}{d\Omega} = |f(\theta)|^2 + |g(\theta)|^2. \quad (13)$$

In case of unscreened nuclei, the scattering reduces to pure Coulomb scattering and equation (1) can then be written as

$$V(r) = \frac{qe^2}{r}. \quad (14)$$

The contributions to scattering amplitudes from V_{sr} become zero and the DCS which is usually referred to as Mott DCS [19] is now given as

$$\frac{d\sigma}{d\Omega} = |f^{(C)}(\theta)|^2 + |g^{(C)}(\theta)|^2. \quad (15)$$

The number of inner phase shifts in (11) and (12) was determined by the convergence criterion. The partial-wave series converge

very slowly for the small angle elastic scattering by ions. To avoid this numerical instabilities in ELSEPA [20] the calculations of scattering amplitudes and DCSs for ions is limited to scattering angles larger than $\sim 1^\circ$.

2.2. The interaction potential

The short range part of the complex optical potential used for the electron ion scattering calculations has the following form [21]

$$V(r) = V_{\text{st}}(r) + V_{\text{ex}}(r) + V_{\text{cp}}(r) - iW_{\text{abs}}(r). \quad (16)$$

Here, $V_{\text{st}}(r)$, $V_{\text{ex}}(r)$ and $V_{\text{cp}}(r)$, the components of the real part of OPM, represent the static, exchange and correlation-polarization potentials respectively and the imaginary part, W_{abs} represents the absorption potential. Within the static-field approximation, the static potential is accurately determined by the nuclear and electronic charge distributions.

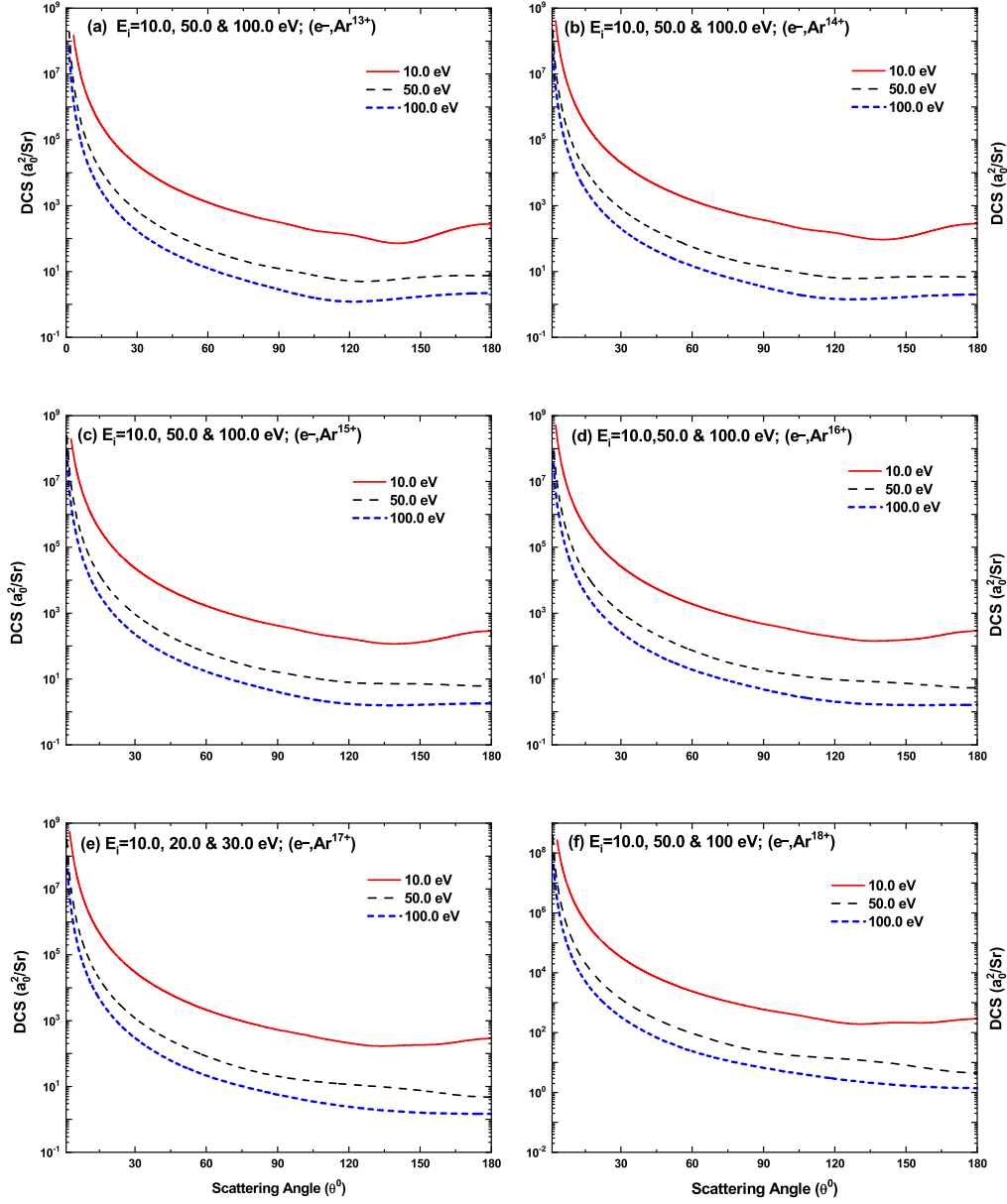


Figure 4. DCS for the elastic scattering of electrons at $E_i = 10, 50$ and 100 eV from (a) Ar^{13+} , (b) Ar^{14+} , (c) Ar^{15+} , (d) Ar^{16+} , (e) Ar^{17+} and (f) Ar^{18+} .

Fermi nuclear charge distribution and analytical electron density, for neutral atom, given by Koga [22] are used in the present calculations. The electron density function is renormalized to the number of electrons of the ion.

Rearrangement collisions occur during the electron scattering due to indistinguishability of projectile and bound electrons. An approximate local potential is used to replace the non-local potential describing the exchange effects. This local potential makes the scattering equations easier to solve numerically and provide accurate calculations at high energies where the exchange effects are comparatively small. In the present work, we use the semi-classical exchange potential of Furness and McCarthy [23]. This is obtained from the non-local exchange interaction using the WKB like wave function.

This exchange potential is given as

$$V_{\text{ex}}(r) = \frac{1}{2}[E_i - V_{\text{st}}(r)] - \frac{1}{2}\{[E_i - V_{\text{st}}(r)]^2 + 4\pi a_0 e^4 \rho_e(r)\}^{1/2}. \quad (17)$$

Here, E_i is the impact energy of the electron and a_0 is the Bohr radius.

The polarization potential that arises from the polarization of the target charge distribution under the action of the electric field of the projectile is given by the Buckingham potential

$$V_{cp,B}(r) = -\frac{\alpha_d e^2}{2(r^2 + d^2)^2}, \quad (18)$$

where α_d is the dipole polarizability of the target atom and d is the phenomenological cut-off parameter which is introduced to avoid singularity at the $r = 0$. Mittleman and Watson [24] suggested

$$d^4 = \frac{1}{2} \alpha a_0 (Z - q)^{-1/3} b_{\text{pol}}^2. \quad (19)$$

Here b_{pol} is an adjustable energy dependent parameter. Considering the fact that the magnitude of the polarization effects decreases as the projectile energy increases, Seltzer [21] suggested the following empirical formula:

$$b_{\text{pol}}^2 = \max\{(E - 50 \text{ eV}) / (16 \text{ eV}), 1\} \quad (20)$$

Excitations of the target occur when the energy lost by the projectile is greater than the first inelastic threshold. This causes a loss of flux from elastic channel to inelastic channel. This loss can be described by the semi-relativistic absorption potential [20]

$$W_{\text{abs}}(r) \equiv \sqrt{\frac{2(E_L + m_e c^2)^2}{m_e c^2 (E_L + 2m_e c^2)}} \times A_{\text{abs}} \frac{\hbar}{2} [v_L \varrho_e(r) \sigma_{bc}(E_L, \varrho_e, \epsilon_1)]. \quad (21)$$

Here m is the mass of the electron, v_L is the velocity of the projectile electron with which it interacts with the bound electrons as if it were moving within a homogeneous electrons gas of density $\varrho_e(r)$ and is given by $v_L = \sqrt{2E_L/m_e}$ corresponding to the local kinetic energy $E_L(r) = E - V_{\text{st}}(r) - V_{\text{ex}}(r)$ and $\sigma_{bc}(E_L, \varrho_e, \epsilon_1)$ is the cross section for collisions involving energy transfer greater than the first excitation energy ϵ_1 of the target atom. In the present calculations, the value of the empirical parameter A_{abs} is taken as 2.

3. Results and discussions

In this paper, ELSEPA code [20] is used to calculate DCSs for elastic scattering of electrons from all the ions of argon isonuclear series. Our calculated DCSs are compared with the experimental data [2–7] and theoretical calculations [2, 4, 5, 13, 14].

In figure 1(a) we present our DCS results for Ar^+ at energy $E_i = 3.3 \text{ eV}$ along with the experimental data of Greenwood *et al* [3]. Our calculations show a good agreement with the data. In figure 1(b), our DCS result for Ar^+ at $E_i = 16 \text{ eV}$ is compared with experimental data and Hatree–Fock calculations of Brotton *et al* [2]. Our prediction shows more or less good agreement with the experimental and theoretical data. In figure 1(c), we compare DCS prediction for Ar^{2+} at the incident energy 16 eV with the experimental data and calculations of McKenna and Williams [4] and Srirangan *et al* [5]. It is seen that our calculations lie more or less close to the above data and calculations. Our calculations predict a minimum at $\sim 72^\circ$ while the measured minimum is witnessed at 85° . Our work can not reproduce the shallow minimum measured at $\sim 55^\circ$. Our calculations and that of Srirangan *et al* [5] show fair agreement with the DCS data for

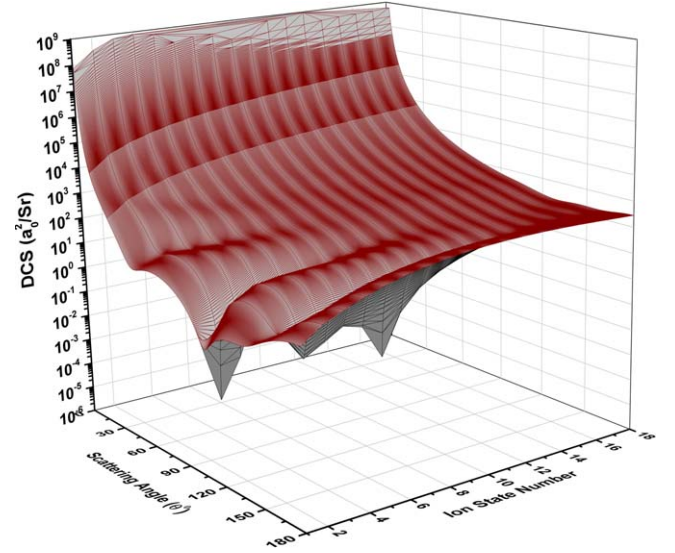


Figure 5. Variation of DCS at 10 eV with the increase of ion charge state.

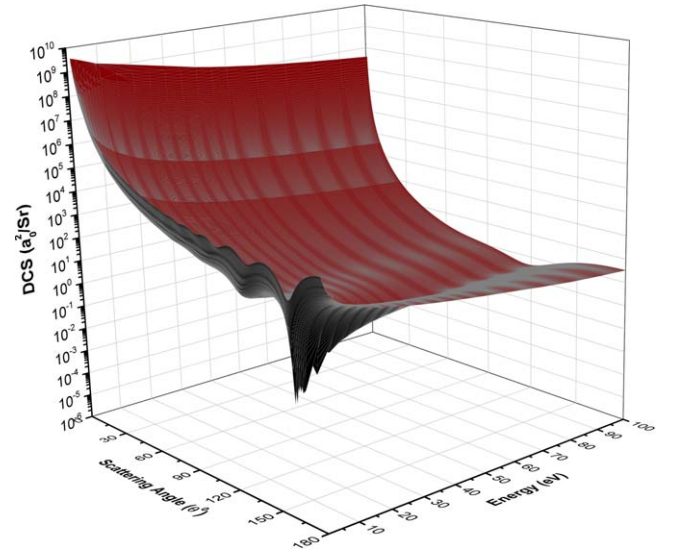


Figure 6. Variation of DCS for Ar^{7+} with the incident energy.

Ar^{3+} at energy 16 eV (figure 1(d)). Both calculations fail to reproduce the shallow interference minimum measured at $\sim 45^\circ$.

In figures 1(e), (f), 2(a) and (b), we display our DCS results at the incident energies 10, 50 and 100 eV for Ar^{3+} , Ar^{4+} , Ar^{5+} and Ar^{6+} respectively. Shifting of minima towards higher angles is observed with the increase of energy. In figures 2(c) and (d), we compare our DCS results for Ar^{7+} at 20 eV and 50 eV along with the calculations of Nishikawa *et al* [14] respectively. These two calculations produce a close agreement with each other except for the minimum regions where the difference of magnitude of the cross-sections is within $\sim 5\%$. We compare our DCS for Ar^{7+} at 100 eV with the measurements of Wang *et al* [6] and the calculations of Nishikawa *et al* [14] (figure 1(e)). Both calculations produce very close agreement with the experimental data. Our

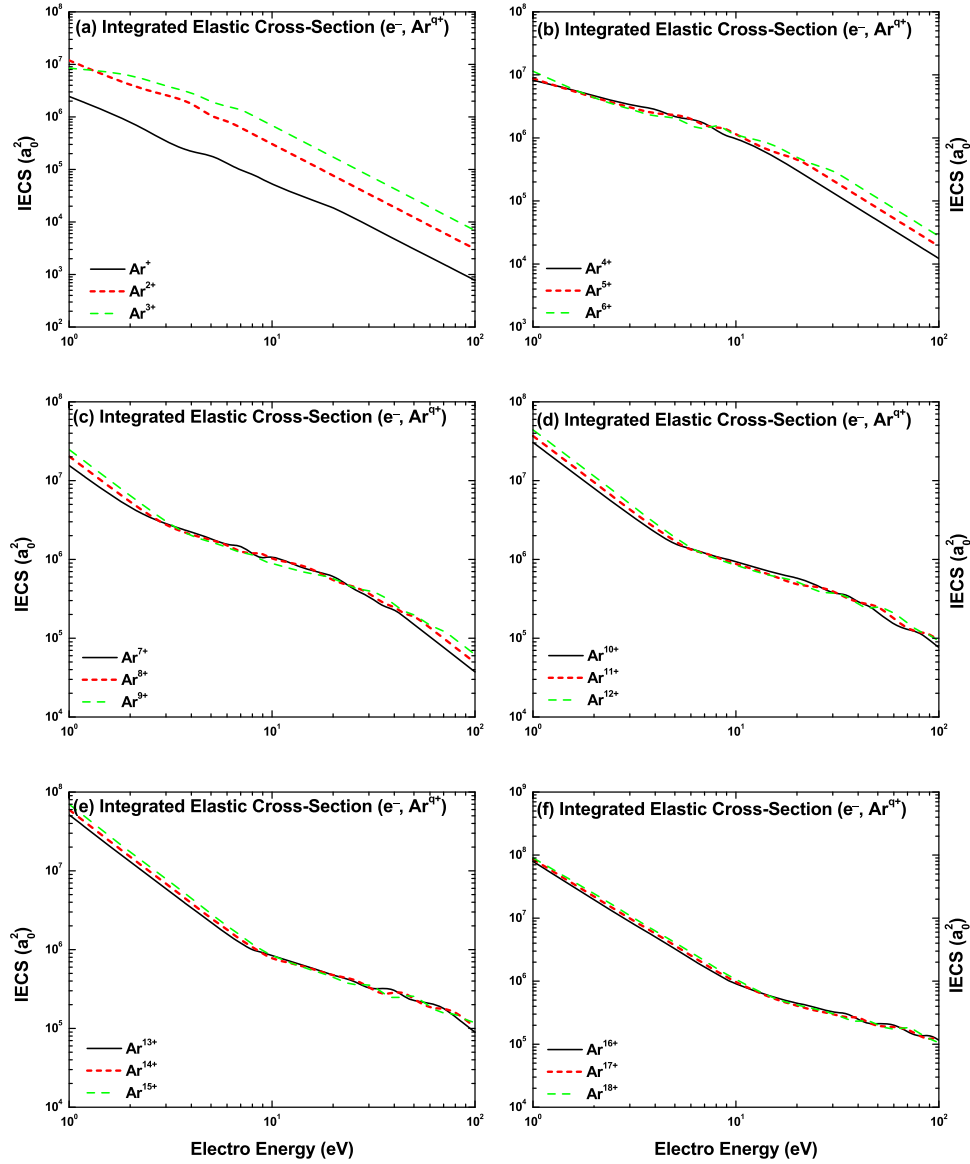


Figure 7. Energy dependence of IECSs for the elastic scattering of electrons from $\text{Ar}^+ - \text{Ar}^{18+}$.

calculations of DCSs for Ar^{8+} at 12.98 eV and 22.46 eV along with the calculations of Shepherd and Dickinson [13] and the experimental data of Bélenger *et al* [7] are presented in figures 2(f) and 3(a) respectively. While both the calculations agree with one another, there are noticeable disagreements with experimental data at the minimum regions at both the energies.

We display the DCSs for Ar^{8+} at 100 eV and for $\text{Ar}^{9+} - \text{Ar}^{17+}$ at energies 10, 50 and 100 eV in figures 3(c)–4(e). In figure 4(f), we present the DCS for bare argon at 10, 50 and 100 eV. We also show the variation of DCS with ion charge states and incident energies in figures 5 and 6 to illustrate the overall interference pattern for different charge states and energies. As seen in the above two figures, the cross section, at a particular energy and angle, increases with the increase of ionic charge in conformity with the Rutherford scattering formula. It is also evident that increasing charge

state weakens the interference pattern. This observation is testified by the experimental data [5, 7]. This is, perhaps, due to the decreasing contributions of short range potential of the bound electrons. The sharp structure in DCS at low energies (figure 6) is due to the interference effect between the scattered waves due to the short range and Coulombic forces. At such low energies, velocity of the incident electron is comparable to the velocities of the bound electrons of the ion, thereby making short range interaction, at small impact parameter, increasingly important.

Figure 7 presents the IECSs of electrons from different charge states of ions. It is apparent from the figure that the cross-section increases with the increase of ionicity. Apart from the figure 7(a), the cross-section does not differ appreciably for the ions of greater degree of ionicity. The apparent differences of cross-sections as in figure 7(a) is due to the screening effect of the surrounding electron cloud. Greater

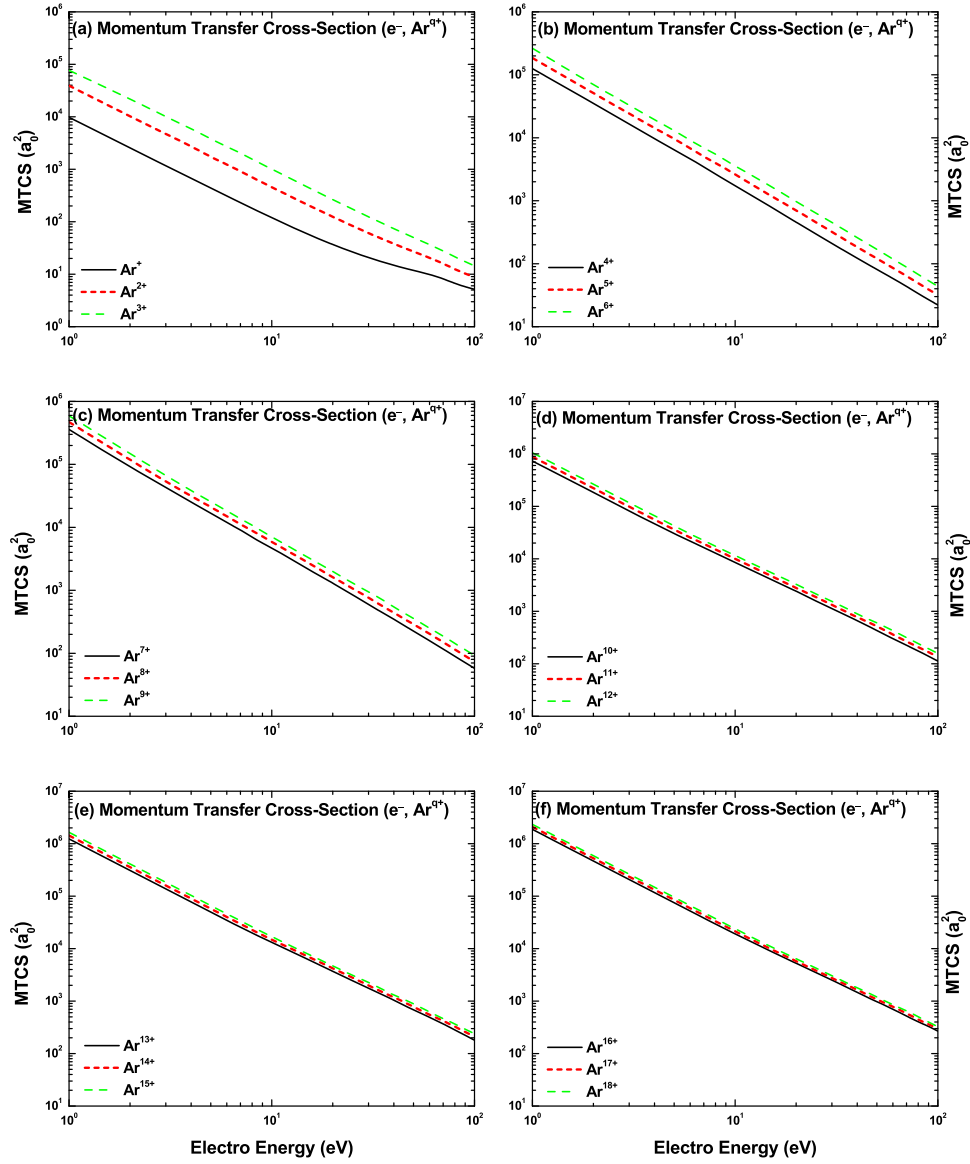


Figure 8. Energy dependence of MTCSs for the elastic scattering of electrons from $\text{Ar}^+ - \text{Ar}^{18+}$.

degree of ionicity results in lesser screening effect of the electron cloud and so increase of cross-section. The interaction potential energy of the projectile electron with bound electron cloud is opposite in sign to that of the nucleus charge. The cross-section for the ions $\text{Ar}^{7+} - \text{Ar}^{17+}$ is almost independent of the degree of ionicity. This is because the cross-section is almost solely determined by the nuclear charge of the ion for higher degree of ionicity, behaving according to the Rutherford scattering formula. Figure 8 shows the energy variation of MTCSs for the ions of the argon isonuclear series. The dependence of the cross-section with the degree of ionicity follows the similar trend to that of IECS.

It is apparent from the DCS of all the ions at the investigated energies, the cross-section is maximum at the forward angle. This is due to the interference of the forward scattering amplitude and the scattered waves and the weak polarization potential.

4. Conclusion

This work presents a description of the elastic scattering of electron off argon ions with different degrees of ionicities. The present calculations of DCSs, IECSs and MTCSs are carried out using a complex optical potential supplemented by the pure Coulomb potential, arising from the ionic charge, in the framework of Dirac partial wave analysis. The work produces a reasonable agreement with the available experimental data and other theoretical calculations. Our result reveals that the cross section increases with the increase of the degree of ionicity of the ion at a particular energy and angle. The sharp structure in the interference pattern for DCSs is also reproduced by the present calculations. This study reveals interference patterns at low and intermediate energies, but higher energies show no maxima–minima in the DCS curves. The monotonic behavior of DCSs at high energies

might be due to the fact that electron interaction time at high energies is very small, thereby reducing the possibility of interference of the scattered waves from the bound electrons. The energy variation of IECSs and MTCSs shows monotonic behavior. Also it is seen that the cross-section is almost independent of the degree of ionicity for ions of Ar^{7+} – Ar^{17+} due to the dominance of the nuclear interaction and reduction of the screening effect of the electron cloud. More experimental data are needed for testing and refining the optical potential and collision dynamics.

Acknowledgments

M Alfaz Uddin acknowledges the financial support from Bangladesh University Grants Commission. Mahmudul H Khandker would like to thank University of Rajshahi for partial funding through project no-5/52/RU/Science-2/18-19.

ORCID iDs

M Alfaz Uddin  <https://orcid.org/0000-0003-3911-0074>

References

- [1] Müller A 1996 Fundamentals of electron-ion interaction *Hyperfine Interact.* **99** 31–45
- [2] Brotton S J, McKenna P, Gribakin G and Williams I D 2002 Angular distribution for the elastic scattering of electrons from $\text{Ar}^{+}(3s\,2\,3p\,5\,2p)$ above the first inelastic threshold *Phys. Rev. A* **66** 062706
- [3] Greenwood J B, Williams I D and McGuinness P 1995 Large angle elastic scattering of electrons from Ar^{+} *Phys. Rev. Lett.* **75** 1062–5
- [4] McKenna P and Williams I D 2001 Differential cross section measurements for elastic scattering of electrons from Ar^{2+} and Xe^{2+} *Phys. Scr.* **2001** 370
- [5] Srigengan B, McKenna P, McGuinness P and Williams I D 1999 Elastic scattering of electrons from argon ions *Phys. Scr.* **1999** 272
- [6] Wang Z, Matsumoto J, Tanuma H, Danjo A, Yoshino M and Kobayashi N 2000 Differential cross section measurements for elastic scattering of electrons by highly charged argon ions *J. Phys. B: At. Mol. Opt. Phys.* **33** 2629
- [7] Bélenger C, Defrance P, Friedlein R, Guet C, Jalabert D, Maurel M, Ristori C, Rocco J C and Huber B A 1996 Elastic large-angle scattering of electrons by multiply charged ions *J. Phys. B: At. Mol. Opt. Phys.* **29** 4443
- [8] McEachran R P and Stauffer A D 2009 Calculation of elastic scattering of electrons from argon using an optical potential *J. Phys.: Conf. Ser.* **194** 042014
- [9] Chen S, McEachran R P and Stauffer A D 2008 *Ab initio* optical potentials for elastic electron and positron scattering from the heavy noble gases *J. Phys. B: At. Mol. Opt. Phys.* **41** 025201
- [10] Bartschat K, Tennyson J and Zatsarinny O 2017 Quantum-mechanical calculations of cross sections for electron collisions with atoms and molecules *Plasma Process. Polym.* **14** 1600093
- [11] Green D G, Ludlow J A and Gribakin G F 2014 Positron scattering and annihilation on noble-gas atoms *Phys. Rev. A* **90** 032712
- [12] Fursa D V and Bray I 2012 Convergent close-coupling method for positron scattering from noble gases *New J. Phys.* **14** 035002
- [13] Shepherd J T and Dickinson A S 1999 Elastic scattering of electrons from positive ions *J. Phys. B: At. Mol. Opt. Phys.* **32** 513
- [14] Nishikawa Y, Kimura E, Kai T, Itikawa Y and Nakazaki S 2004 Elastic scattering of electrons from Na-like ions *J. Phys. Soc. Japan* **73** 348–52
- [15] Rose M E 1961 *Relativistic Electron Theory* (New York: Wiley)
- [16] Salvat F, Fernández-Varea J M and Williamson W Jr 1995 Accurate numerical solution of the radial schrödinger and dirac wave equations *Comput. Phys. Commun.* **90** 151–68
- [17] Mott N F *et al* 1965 *The Theory of Atomic Collisions* vol 35 (Oxford: Clarendon)
- [18] Walker D W 1971 Relativistic effects in low energy electron scattering from atoms *Adv. Phys.* **20** 257–323
- [19] Mott N F 1929 Nf mott, proc. roy. soc.(london) a124, 425 (1929) *Proc. R. Soc.* **124** 425
- [20] Salvat F, Jablonski A and Powell C J 2005 Elsepadirac partial-wave calculation of elastic scattering of electrons and positrons by atoms, positive ions and molecules *Comput. Phys. Commun.* **165** 157–90
- [21] Salvat F 2003 Optical-model potential for electron and positron elastic scattering by atoms *Phys. Rev. A* **68** 012708
- [22] Koga T 1997 Analytical hartree-fock electron densities for atoms He through Lr *Theor. Chim. Acta* **95** 113–30
- [23] Furness J B and McCarthy I E 1973 Semiphenomenological optical model for electron scattering on atoms *J. Phys. B: At. Mol. Phys.* **6** 2280
- [24] Mittleman M H and Watson K M 1960 Effects of the pauli principle on the scattering of high-energy electrons by atoms *Ann. Phys., NY* **10** 268–79